Método sin malla para el estudio de la terapia fototermal en tumores cancerígenos bidimensionales

A meshless numerical method to study plasmonic photothermal therapy in two-dimensional cancer tumors

DOI: https://dx.doi.org/10.17981/ingecuc.21.2.2025.12

Artículo de Investigación Científica.

Fecha de Recepción: 23/07/2023, Fecha de Aceptación: 16/12/2024.

Juan Felipe Hurtado-Álvarez
Universidad Pontificia Bolivariana, Medellín, Colombia
juanfelipeh2000@gmail.com

Raúl Adolfo Valencia-Cardona
Universidad Pontificia Bolivariana, Medellín, Colombia
raul.valencia@upb.edu.co

Carlos Andrés Bustamante-Chaverra
Universidad Pontificia Bolivariana, Medellín, Colombia
carlos.bustamante@upb.edu.co

Whady Felipe Flórez-Escobar
Universidad Pontificia Bolivariana, Medellín, Colombia
whady.florez@upb.edu.co

To cite this paper
J. Hurtado-Álvarez, C. Bustamante-Chaverra, R. Valencia-Cardona & W. Flórez-Escobar "A meshless numerical method to study plasmonic photothermal therapy in two-dimensional cancer tumors," INGE CUC, vol. 21, no. 2, 2025. DOI: https://dx.doi.org/10.17981/ingecuc.21.2.2025.12

Resumen

Introducción: La terapia fototermal plasmónica (PPTT) con nanopartículas metálicas ha ganado relevancia como alternativa menos invasiva en el tratamiento de tumores cancerígenos del tipo adenocarcinoma. La PPTT utiliza radiación láser para generar efectos plasmónicos en las nanopartículas distribuidas en el tejido cancerígeno, lo que resulta en hipertermia y muerte celular por apoptosis.
Objetivo: Obtener distribuciones de temperatura y a partir de esta, distribuciones bidimiensionales de daño celular en tejidos tumorales sometidos a PPTT.
Metodología: Se implementa una metodología numérica basada en funciones de base radial (RBF) para la solución de la ecuación de Pennes o biocalor y los modelos de Arrhenius y de tres estados para la estimación de la muerte celular. La metodología numérica desarrollada, validada y aplicada está basada en el método de soluciones particulares aproximadas en formulación local (LMAPS).
Resultados: Se demuestra la capacidad del método de solucionar problemas con fuentes variables, regiones múltiples y diferentes tipos de condiciones de fronteras mediante la comparación con la herramienta computacional OpenFOAM basada en volúmenes finitos y resultados numéricos reportados por otros autores. Esto se realiza a partir de la solución de situaciones hipotéticas de transferencia de calor en tejidos incluyendo dominios 1d y 2d con fuentes metabólica, término de perfusión y conversión térmica de la radiación del láser.
Conclusiones: Mediante una situación de PPTT en tejido superficial, se aplica la metodología numérica desarrollada desde la descripción de distribución de energía aportada por el láser hasta la estimación de los porcentajes locales de muerte celular. Esta metodología numérica es la base para el análisis, optimización y diseño de procesos de aplicación de PPTT en ambientes clínicos considerando su potencial para resolver geometrías complejas, condiciones de frontera y parámetros variables en el tiempo y dominios con múltiples regiones.

Palabras clave: Ecuación de biocalor; Terapia fototermal plasmónica; nanopartículas de oro; funciones de base radial, LMAPS, muerte celular.

Abstract

Introduction: Plasmonic photothermal therapy (PPTT) with noble metal nanoparticles (NPs) have gained great relevance as less invasive platforms in the treatment of adenocarcinoma-type cancer tumors. The PPTT uses laser radiation to generate plasmonic effects in NPs that are distributed in the cancerous tissue, producing hyperthermia and cell death by apoptosis.
Objective: To obtain two-dimensional temperature distributions and the associated cell damage distributions in tumoral tissue subjected to PPTT.
Method: A numerical methodology based on Radial Basis Functions (RBFs) is implemented for solving the Pennes or bioheat equation and the Arrhenius and Three-state models for cellular damage estimation. The developed, validated and applied numerical methodology is based on the method of approximate particular solutions in local formulation (LMAPS).
Results: The capability to solve problems with variable sources, multiple regions and different types of boundary conditions is shown by the comparison with OpenFOAM computational tool based on finite volume method and numerical results reported in the literature. This is performed by solving hypothetical situations of heat transfer in tissues including 1D and 2D domains with metabolic sources, perfusion term and radiation thermal conversion.
Conclusions: The developed methodology is applied to a situation of PPTT in superficial tissue, from laser energy distribution description to the local percentage of cellular damage. This numerical methodology is the basis of the analysis, optimization and design of PPTT application processes in clinical environments considering its potential to solve complex geometries, time-varying boundary conditions and parameters and domains with multiple regions.

Keywords: Bioheat equation; Plasmonic photothermal therapy; gold nanoparticle; radial basis functions, LMAPS, cellular damage.

INTRODUCCIÓN

New therapies based on photothermal treatments with noble metal nanoparticles (NPs) have gained great relevance as less invasive platforms that make it possible to improve effectiveness and reduce side effects in the treatment of adenocarcinoma-type cancer tumors [1] [2]. These treatments, known as plasmonic photothermal therapy (PPTT), use laser radiation to generate plasmonic effects in NPs that are distributed in the tissue, producing hyperthermia. PPTT can reduce side effects of traditional therapies because it is a selective alternative that produces focalized heat generation and prevents damage in healthy cells. Regarding the modeling and simulation of processes related to the treatment of adenocarcinomas by PPTT, work has been carried out mainly on finding temperature distribution on the tumor tissue subjected to irradiation [3] [4]. The heat transfer model proposed by Pennes [5] to study the temperature distribution in human forearm tissue, known as the bioheat equation, has become the transient heat conduction model in tissues. It includes chemical energy conversion into metabolic heat and thermal effect of blood circulation in the tissue usually known as perfusion. The reliability of Pennes equation results with respect to experimental measurements depends on the correct estimation of the properties involved such as thermal conductivity, density, heat capacity and perfusion rate in tissue [6]. This is verified by the abundance of verified numerical results that have been found for temperature distributions in different tissues using a wide variety of numerical methods, boundary conditions and modifications of the original equation [7] [8] [9].

In the case of PPTT with NPs, the Pennes equation has been modified in order to consider both the indirect effect of irradiation given the presence of nanoparticles and the direct effect on the tissue. Tjahjono and Bayazitoglu [10], using an approximation in a one-dimensional domain, obtain solutions for the radiative transfer equation (RTE) for a transparent test material (polydimethylsiloxane-PMDS) embedded with gold nanoshells. Once the heat flux by radiation at each point of the tissue is obtained, a variation of the one-dimensional Pennes equation is solved by finite differences to calculate the temperature distribution. Vera and Bayazitoglu [11] employ the developed one-dimensional model and solution procedure presented in [10] to computationally analyze radiation and heat transfer in tissue embedded with homogeneous distributions of gold NPs and surrounded by healthy human tissue without NPs. By examining properties of five tissues (Breast, Brain, Subcutaneous Fat, Liver and Skin), they show, based on numerical results, that NP decreases heating time and increases tissue energy absorption. Increasing laser power can cause a temperature difference such that the laser entry zone would undergo pyrolysis and ablation while the farthest zone would remain at the initial temperature. Likewise, they suggest that the use of two lasers at each end of the area to be irradiated can flatten the temperature distribution around a maximum value in the center of the target area, improving the application of the therapy. However, the simplifications made in this work, such as the one-dimensional domain, the use of constant optical and thermal properties of healthy tissue and the absence of perfusion, implies that results do not approximate a real PPTT case. In relation to the above simplifications, the work of Feng et al. [12] offers evidence on key aspects in the simulation of tissues subjected to irradiation. Through the solution by the finite element method of the three-dimensional Pennes equation and the estimation of the heat generated in the tissue by the Monte-Carlo method for the irradiation term, the authors obtain a temperature distribution close to measurements in irradiation experiments of pancreatic tumors in laboratory mice with NP administered via vascular route. Obtaining this numerical solution was only possible from the implementation of a methodology for temporal tuning of properties, demonstrating that the correct modeling of tissues subjected to irradiation depends largely on the proper estimation of thermal conductivity, blood perfusion and the absorption and dispersion coefficients as a function of temperature. More recently, Motaei et al. [13] propose a transient one-dimensional model for cancer tissue subjected to PPTT that includes temperature-dependent properties and photo-thermal-mechanical interactions by considering non-Fourier heat conduction effects and Zener-type thermo-viscoelastic model. Although the authors propose a comprehensive model that can reproduce acoustic waves generated by heating-induced oscillations, the methodology is not quantitatively validated and is restrictive to one-dimensional geometries. Xu et al. [14] extrapolate the applicability of the model of Vera and Bayazitoglu [11] to the

two-dimensional case in cylindrical coordinates and to tissues that are inside the body, far from the skin, as in the case of the liver tumor. The authors conclude that the temperature distribution depends on the retention ratio, defined as the ratio between the concentration of NP in the tumor and that of NP in healthy tissue. They find, in the specific case studied, that ratios less than 4 can cause unfavorable damage and, in consequence, it is necessary to carry out more simulations for other combinations of NP and tissues in order to have a better description of the relationship between irradiation parameters and thermal processes before experimental procedures. Huang et al. [15] employ a simplified model of the Pennes equation to simulate the transient temperature distribution in a cylindrical test material embedded with pancreatic cancer cells and gold nanorods. The authors report consistent experimental measurements and numerical results from an exponential radiation model in terms of optical density, which, in turn, is a function of NP concentration. Despite being an in vitro case and a model that does not solve RTE or include perfusion, the work establishes a methodology for estimating cell death from irradiation using an Arrenius-type model. As future work, the authors propose the study of the flow of nanoparticles in tissues, as well as non-homogeneous distributions, resulting from cell-NP interactions. In this sense, Soni and Sinha [16] identify zones of thermal ablation from numerical results in a cylindrical tumor surrounded by healthy tissue and embedded with determined concentrations of gold NPs, such as those enclosed by the 55°C isothermal line. From simulations carried out with a simplified RTE model and the Pennes equation with constant coefficients, they obtain intensity radiation and time required to cause thermal ablation in a tumor with diameter between 20 and 40 mm. With a similar numerical methodology, Shaw et al. [17], study PPTT with Indocyanine green (ICG) in cylindrical geometries for different spatial distributions of ICG according to delivery procedures. Even though they obtain irradiation times to cause thermal damage in tumor tissue and find good agreement with finite difference results, the numerical methodology based on Lattice Boltzmann method (LBM) is restricted to simple two-dimensional geometries and further work may be performed to tune parameters in the proposed scheme.

After the development of the Kansa method [18], radial basis functions (RBFs) have been widely used to solve partial differential equations (PDEs). The Kansa method is a meshless approach where an RBF approximation to the solution is collocated at a set of nodes distributed on the domain and it has been widely applied to a variety of PDE such as convection-diffusion, Helmholtz, Poisson and Laplace in several contexts. However, global collocation methods for practical problems have been described by Robert Schaback [19] to be affected by an uncertainty relation: high conditioning is associated with low accuracy, and high accuracy is associated with low conditioning. Because of this reason, the local implementation of RBF collocation schemes such as the Method of Approximate Particular Solutions (MAPS) allows a practical and straightforward application for solving transport phenomena equations. In addition, the nature of this technique has attractive features such as mesh-free basis, high order approximation of variables and versatility in the application of boundary conditions compared to other methods like finite differences (FDM), finite volumes (FVM), finite elements (FEM) and Boundary elements (BEM). Among the strategies to prevent ill-conditioning in the RBF collocation method, two approaches have been successfully implemented: local implementation and indirect RBF methods. Lee et al [20] propose the local approximation for a multi quadratic (MQ) scheme, in which only nodes that are in the subdomain of influence of a central node are used in the asymmetric method to solve Poisson's equation. This work serves as the basis for Sarler and Vertnik [21] to create an explicit scheme to solve the transient diffusion equation. More recently, other schemes are implemented by modifying traditional methods using the symmetric and asymmetric collocation, for example, Moroney and Turner [22] apply an RBF interpolation in FVM to reconstruct gradients in non-linear 2D and 3D diffusion problems by using the asymmetric method.

Recently, Chen et al. [23] propose the MAPS which is an integrated RBF method for the case of a PDE whose differential operator, or only part of it, can be given in terms of radial components of polar and spherical coordinate systems. For this case, the authors proposed to approximate the radial component of an PDE in terms of an RBF interpolation and, by integrating the resulting non-homogeneous ordinary differential equation, obtain an approximate representation of the field variable through a linear superposition of the

corresponding particular solutions. However, computational efficiency is a limiting aspect since the global interpolation matrix is fully populated and consequently the solution of the resulting system of equations takes much more time compared to local strategies. In this regard, MAPS has been applied to several PDE problems such as Poison [26] [25], Helmholtz [26] and Navier-Stokes equations [27], and accurate localized formulations has been implemented to solve Poisson [28], convection-diffussion equations [29] and, more recently, Navier-Stokes equations [30]. However, the local MAPS (LMAPS) scheme has not yet been applied to solve Bio-heat equation including multi-zone, Robin-type boundary conditions and multiple variable source terms as they appear in PPTT modelling. In this sense, LMAPS allows to have a high order approximation with less ill-conditioning issues than traditional RBF methods [28], and a potential application to complex geometric shapes whereby mesh-based method can be required dense meshes, produce numerical oscillations or decrease global accuracy [30]. Although mesh-based methods have been successfully applied to model irregular geometries of real tumors, LMAPS implementation can reduce effort in mesh generation and adaptation, simplifying the preprocessing stage and handling complex boundaries with greater ease.

The use of noble metal NPs in the implementation of PPTT plays a fundamental role both in the production of heat on the surface of the nanostructure due to the generation of localized plasmonic resonances, as well as in the selection of the appropriate optical window to prevent the absorption of electromagnetic radiation by the healthy tissue. In particular, the frequency of electromagnetic radiation whereby the system is excited depends mainly on the geometry and the medium in which the NPs are immersed. The aim of this work is to develop, validate and apply an LMAPS-based numerical methodology to obtain temperature and cell damage distributions from the solution of the Bioheat equation and for estimating cell death with the Arrhenius and three-state models. The capability of the method is demonstrated by solving several hypothetical situations of heat transfer in tissues with variable sources, multiple regions, different types of boundary conditions and by comparing with the OpenFOAM tool and with numerical results reported by other authors.

MATHEMATICAL MODELS

Bioheat equation

Modelling heat transport and temperature distribution for thermal therapies at the tissue level is a challenge due to convective effects of blood flow, metabolic processes and laser tissue interaction [31]. One of the most used bioheat models is the Pennes bioheat equation (1), which provides an internal energy balance in terms of temperature and the contribution of the above mechanisms.

$$k\nabla^2 T + \eta_b \rho_b c_{pb}(T_a - T) + Q_m + Q_s = \rho c_p \frac{\partial T}{\partial t} \quad (1),$$

where T is the temperature; k, p and cp are the thermal conductivity, density and the specific heat of the medium; η_b,ρ_b, cp_b blood perfusion, density and the specific heat of blood; T_a corresponds to the basal temperature; Q_m and Q_s are the metabolic heat generation of tissue and the distributed volumetric heat source by nanoparticles. In the case of in vitro simulations, the term for blood perfusion is omitted, while the term for metabolic heat generation is also omitted in the case of non-cellular simulations.

The presence of nanoparticles in the tumor can increase the tissue temperature due to the heat generated by the plasmonic effect. The heat generation of individual nanoparticles can be described as follows:

$$Q_{\text{nano}} = C_{\text{abs}} \times I \quad (2),$$

with C_{abs} as the absorption cross section area and I the laser intensity. For a cluster of nanoparticles, the heat generated can be estimated as:

$$Q_s = N \times Q_{\text{nano}} \quad (3).$$

At the macroscopic scale, equation (2) is modified to include the laser variation as a function of the geometry and optical properties of the irradiated sample. To describe the laser interaction with tissues, Soni et al [32] use the Beer-Lambert law in terms of the sample height and its absorption (α) and scattering (β) coefficients, defined as follows:

$$Q_s(z) = \alpha I_0 \exp[-(\alpha + \beta)z] \quad (4).$$

Also in tissues, Welch et al [33] improved the Beer-Lambert model by including the radial distribution of laser power according to a Gaussian profile with laser beam constant σ(o) and given by the following equation:

$$Q_s(r,z) = \alpha I_0 \times \exp\left[\frac{-r^2}{2\times\sigma^2(0)\times\exp(\beta z)}\right] \times \exp[-(\alpha+\beta)z] \quad (5).$$

For a highly scattering medium, Sahoo et al. [34] propose a modification of the Welch model in accordance with experimental observations in a tissue-like sample, as shown in the following expression:

$$Q_s(r,z) = \alpha I_0 \times \exp\left[\frac{-r^2}{2\times\sigma^2(0)\times\exp(\beta z)}\right] \times \exp(-\alpha z) \times \{1-\exp(-\beta z)\} \quad (6).$$

The difference between the Welch model (5) and the Sahoo model (6) is that the latter considers backscattering, which means that the maximum heating does not occur at the top. However, equation (6) does not work for low scattering media because scattering coefficient (ß) tending to zero would make the expression negligible.

Cell damage model

Regarding the cell death model, two options are considered: the Arrhenius model, also presented in [32], and the O'neill three-state model [35]. In the first case, equation (7) is used to estimate the damage factor k as a function of temperature. The time integral is calculated from the temperature time series obtained in the respective simulations. The equation parameters *A* and *Ea* depend on the cell type; in this case, the values reported in [32] were used. Cell damage is predicted from two states, live cells where the damage factor is less than 1 and dead cells in the opposite case, which serves to differentiate areas where the treatment has caused cell death.

$$k(t) = \int_0^t \exp\left\{-\frac{\mathrm{Ea}}{RT(t')}\right\}dt' \quad (7).$$

The three-state model uses two ordinary differential equations to estimate the relative population of cells in a given state in a representative volume of the domain. Thus, the relative population of alive (A), dead (D) and vulnerable (V) cells can be calculated using equations (8), (9) and (10). The temperature-dependent coefficient kf estimates the rate of cell death, while the coefficient kb corresponds to the rate of recovery of vulnerable cells.

$$\frac{dA}{dt} = -k_f \times A + k_b \times (1-A-D) \quad (8),$$

$$\frac{dD}{dt} = -k_f \times (1-A-D) \quad (9),$$

$$A + D + V = 1 \quad (10).$$

RADIAL BASIS FUNCTION COLLOCATION METHODS

As part of meshless methods, the RBF collocation approach is very attractive for solving the bioheat equation because it can be applied to complex geometries without considerable accuracy lost [23]. Also, interpolation strategies and local flux evaluations can be easily applied in the framework of RBF methods in order to treat multizone problems such as in the case of a tumor surrounded by healthy tissue. Among the RBF collocation methods, two approaches are used here to solve the Bioheat equation: RBF local direct collocation (LRBF) and the local Method of approximate particular solutions (LMAPS).

Bioheat equation

The Bioheat equation together with temperature (Dirichlet), heat (Neumann) or convective heat (Robin) boundary conditions can be expressed as a linear boundary value problem of the following form:

$$L[T] = f(\overline{x}) \quad (11),$$

$$B[T] = g(\overline{x}) \quad (12),$$

where L and B are the internal and boundary differential operators, defined by governing equation (1) and boundary conditions given according to the case. To solve this problem by local RBF collocation, a nodal distribution must be set throughout the domain, and local stencils (circles) must be defined as shown in Figure 1 for an arbitrary geometry.

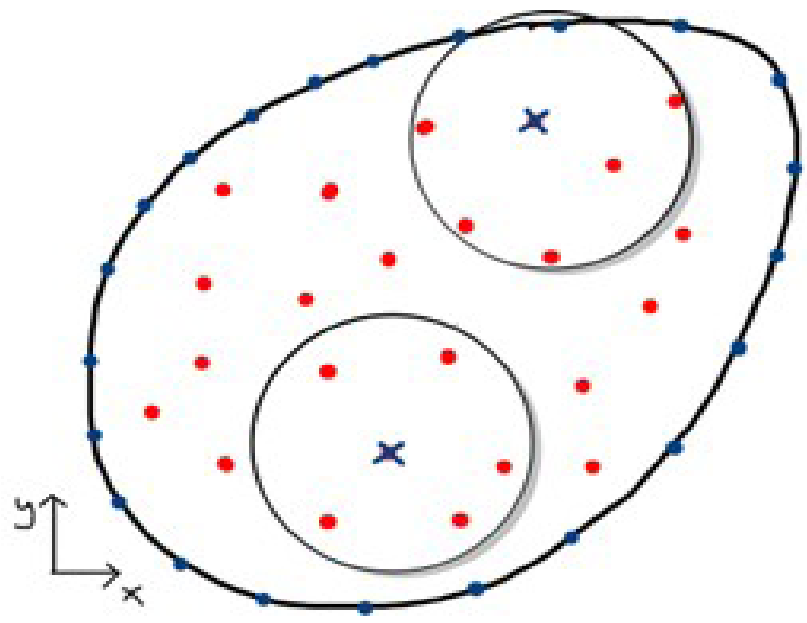

Fig 1. Nodal distribution and stencils for an arbitrary geometry.

If *Ns* is the number of points in the stencil, an RBF approximation for the dependent variable T is proposed as the following linear combination,

$$T(\overline{x}) = \sum_{i=1}^{N_s} \alpha_i \psi(r_i) + P_m \quad (13),$$

where α_i are the collocation coefficients and is an RBF evaluated at the Euclidian distance between evaluation point and a trial point is r_i. P_m is an m-degree polynomial added by some authors to improve the conditioning of the resulting collocation matrix, with m as the order of the RBF, according to its type. In this work, no polynomial term is added since it does not represent an improvement in terms of accuracy. Multiquadric (MQ) equation is employed, which also depends on the shape parameter c that must be set before computation. The effect of this parameter on solution is analyzed in the numerical result section. Equation (13) can be evaluated at each of the *Ns* nodes of the stencil with the aim of obtaining the following local system of equation:

$$[T]_s = [\psi][\alpha] \quad (14),$$

where column vector *[T]s* contains unknown temperature values at stencil nodes and [ψ] is a *Ns x Ns* symmetric matrix obtained by RBF collocation at the stencil nodes. Therefore, a relation between unknown temperatures and interpolation coefficient is obtained as:

$$[\alpha] = [\psi]^{-1}[T]_s \quad (15).$$

On each stencil, local nodal index must have assigned a global nodal index to assemble the global matrix. To obtain a global formulation from local stencil interpolations, variable approximation (13) is substituted into governing equation and boundary condition expressed in the concise form (11) and (12), respectively. Then, coefficients are replaced by its definition in terms of unknown temperature to obtain the following equations:

$$L[T] = [L[\psi]][\psi]^{-1}[T]_s = f(\overline{x}) \quad (16),$$

$$B[T] = [B[\psi]][\psi]^{-1}[T]_s = g(\overline{x}) \quad (17).$$

Finally, the global ensemble is expressed in the form of matrix equation (18) with *[A]* containing the coefficients that multiply the variable T in the positions of the local nodes (columns) after applying the operators L and B at each node of the domain (rows). Matrix *[B]* contains the forcing functions, where *f(x)* and *g(x)* represent the functions for the internal nodes and boundary nodes, respectively. By solving this global linear system, the solution column vector *[T]* is found with temperatures at all points of nodal distribution.

$$[A][T] = [B] \quad (18).$$

Local method of approximate particular solutions (LMAPS) for steady and transient problems

As in the RBF collocation method, subdomain or stencil nodes are also used to define an approximation. LMAPS is formulated locally according to equation (20) where coefficients α are unknown weight factors and *Ns* is the number of neighboring nodes in the stencil. Unlike RBF method, represents the particular solution of the governing equation symmetric part that in this case corresponds to the Poisson problem with the RBF ψ as forcing term.

$$\nabla^2 \phi = \psi \quad (19),$$

$$T(\overline{x}) = \sum_{i=1}^{N_s} \alpha_i \phi(r_i) \quad (20).$$

In this case, equation (14) is not expressed in terms of RBF matrix but in terms of the particular solution matrix [ϕ] as it is given by (21).

$$[T]_s = [\phi][\alpha] \quad (21).$$

The rest of the procedure to obtain a linear equation system in terms of dependent variable (equation (18)) is similar to RBF collocation method, except in the definition of internal operator *L*. As mentioned, equation (19) only approximates the symmetric part of operator, then any linear operator can be decomposed in a symmetric and non-symmetric part as *L=Lr+Lx*. Therefore, when the operator is applied to the particular solution, equation (22) is obtained according to the auxiliary problem definition given by equation (19).

$$L[T] = [\psi + L_x[\phi]][\phi]^{-1}[T]_s = f(\overline{x}) \quad (22).$$

Particular solutions ϕ are given by the analytical solution of equation (19). Here, MQ RBF is used as forcing function in equation (19) and after double integration in terms of r and some simplifications, the following expression is obtained.

$$\phi(\bar{r}) = \tfrac{1}{9}\left(4 \times c^2 + r^2\right) \times \psi - \tfrac{c^3}{3} \times \ln(c + \psi) \quad (23).$$

Temporal discretization: θ-scheme

To solve the transient problems with the scheme described above, several options can be implemented because equation (1) is in fact an initial value problem. In this case, θ-scheme is used with the governing equation expressed as (24) with its symmetric part L defined by (25).

$$\rho c_p \tfrac{dT}{dt} = L[T] + Q_m + Q_R + \eta_b \rho_b c_{pb}[T_a] \quad (24),$$

$$L[T] = k\nabla^2 T - \eta_b \rho_b c_{pb}[T] \quad (25).$$

In this scheme, time derivative is expressed as a finite difference, and right-hand side terms are evaluated at the unknown present temperature values (*n+1*) and past temperature values (*n*) according to the weigh parameter θ, as it is shown in equation (26). Hence, if θ=0, the scheme becomes explicit or Euler scheme and with θ=1, the scheme is fully implicit.

$$\rho c_p \tfrac{T^{n+1}-T^n}{\Delta t} = \theta\left(L\left[T^{n+1}\right] + {Q_m}^{n+1} + {Q_R}^{n+1} + \eta_b \rho_b c_{pb} {T_a}^{n+1}\right) + (1-\theta)(L[T^n] + {Q_m}^{n} + {Q_R}^{n} + \eta_b \rho_b c_{pb} {T_a}^{n}) \quad (26).$$

In summary, LMAPS implementation is broken down into the following steps:

- Local interpolation matrices are obtained for each of the stencils according to equations (16) and (17), regarding definition of the internal differential operator L given by (22) and the boundary operator B given by fixed boundary conditions.

- Global system of equations (18) is assembled by imposing the equation (26) at each internal node and the corresponding boundary condition at each boundary node.

- For each time step, equation system (18) is solved to obtain solution vector Tn+1 after updating values from last time step in the vector Tn.

ScalarTransportFoam mathematic model

The scalarTransportFoam is a basic solver from OpenFOAM software which resolves a transport equation for a passive scalar, using a user-specified stationary velocity field. A typical application is a scalar convection-diffusion problem solution for a given velocity field. This solver implements and solves a convection-diffusion scalar transport equation with options to add source terms, user-specified boundary conditions and an arbitrary velocity field provided by the user and read at runtime. Besides, the main limitations of the solver are the diffusion coefficient is assumed to be a constant scalar [36] [37]. The scalarTransportFoam solver uses a complete convection-diffusion equation, in the following form:

$$\frac{\partial T}{\partial t} + \nabla \cdot (U \times T) - \nabla^2 (D_T \times T) = Q_s \quad (27),$$

where T is the transported scalar (corresponding to temperature here), U is the fluid velocity, and D is the diffusion coefficient divided by the fluid density, both supposed to be constant. In this work, U is made null since no movement is considered in the domain, and Q_s is the source term, that can be given in terms of (4), (5) or (6) for laser irradiation. In bioheat equation, this term also contains metabolic and perfusion heat.

NUMERICAL RESULTS

The results of different numerical cases including 1D and 2D domains with metabolic sources, perfusion term and thermal conversion of laser radiation are presented below. The first case is solved in a 1D domain without radiation term; the second problem is a 2D geometry with healthy and tumor tissue regions, and the third case also includes multiple regions, but the tumor region contains NPs. Additionally, in this last case, the cell death factor is estimated with Arrhenius and three state models.

One-dimensional heat transfer in tissue

In order to evaluate the feasibility of using the OpenFOAM tool to solve the Pennes equation (1), the 1D problem in tissue without radtion source proposed by Zhang et al. [31] is solved.

For this case, a 1D geometry was used with one boundary with an adiabatic condition (Neumann) and another with an isothermal condition (Dirichlet), as shown in Figure 2.

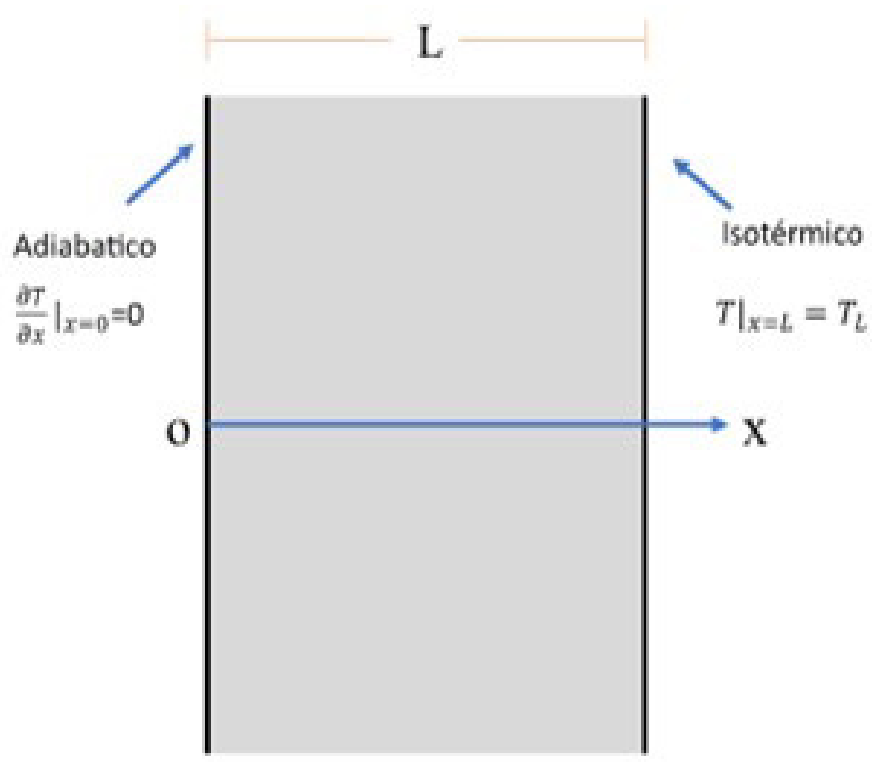

Fig 2. Geometry and boundary conditions for heat transfer problem in tissue proposed by Zhang et al. [31].

The bioheat equation (1) is used, so that Qs = 0 W/m3, since laser radiation sources are not considered, and with:

$$Q = \eta_b \rho_b C_{pb} \times (T_e - T) \quad (28),$$

$$T_e = T_a + \frac{Q_m + Q_s}{\eta_b \rho_b C_{pb}} \quad (29).$$

The analytical solution for this problem is given by the following equation:

$$T(x,t) = T_e + \frac{2\times\alpha}{L}(T_L - T_e)\sum_{m=1}^{\infty}(-,1)^{m-1}\beta_m \cos(\beta_m x)\frac{1-\exp\left[-\left(\alpha{\beta_m}^2+\eta*\right)t\right]}{\alpha{\beta_m}^2+\eta*} \quad (30),$$

Where $\beta_m = \frac{(m-0.5)\times\pi}{L}$ .The thermal and geometric properties are observed in Table 1, as proposed in [31].

TABLE 1. PARAMETERS USED IN THE CASE OF TEMPERATURE DISTRIBUTION IN 1-D TISSUE.

Parameter	Value	Unit
k	0.5	W m-1 K-1
ρ = ρb	1052	kg m-3
Cp = Cpb	3800	J kg-1 K-1
ηb	1x10-4	s-1
Qm	400	W m-3
Ta	37	° C
L	0.04	m
TL	30	° C

Numerical results are obtained with LMAPS, LRBF and openFOAM scalarTransportfoam solver, and their accuracy is assessed with respect to the analytical solution (30).

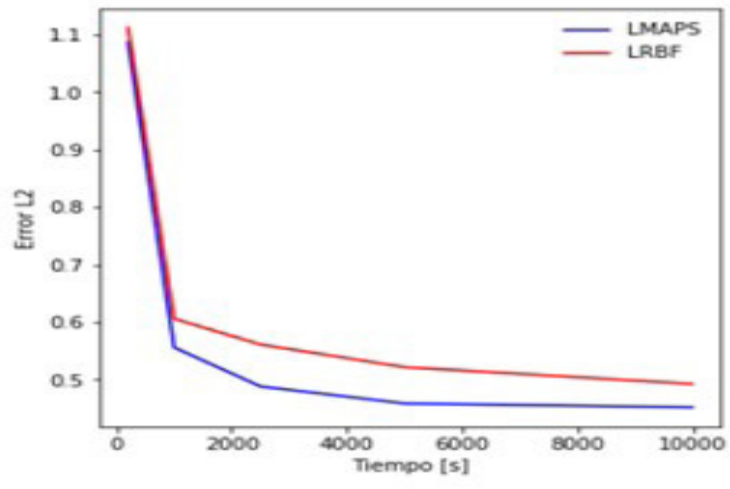

Fig 3. Error L2 norm comparison between LMAPS and LRBF with respect to the analytical solution for heat transfer problem in tissue.

Figure 3 shows that the error obtained with the LMAPS method remains lower than the error obtained by the LRBF method throughout the simulation time; it is for this reason that LMAPS is chosen to provide solutions for the next study cases. Figure 4 presents OpenFOAM and LMAPS results in comparison with the analytical solution given by (30) for different times.

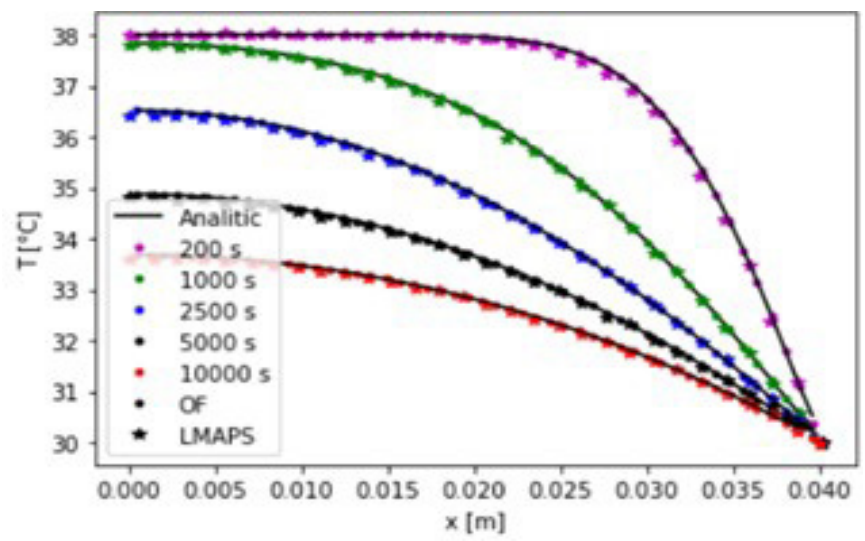

Fig 4. Temperature distribution for heat transfer in 1-D tissue with openFOAM and LMAPS.

As can be seen in Figure 4, the numerical results of both methods agree with the analytical solutions for the comparison times, thus validating the treatment of the transient term of the bioheat equation.

Two-dimensional heat transfer in tissue with tumor

In order to evaluate the LMAPS capability to obtain accurate results in problems with multiple regions and heat sources, the following two-dimensional problem is proposed according to [31]. As it is shown in Figure 5, the solution domain includes healthy tissue and tumor zones. The latter has dimensions $L/4 \times L/4$ where L is half length of total domain. This definition agrees with symmetry condition imposed in $x=0$ and, in consequence, the redefinition of the domain as the half part of the geometry shown in Figure 5. On the upper boundary, heat loses by natural convection with surrounding air are imposed by a Robin type condition; on the lower boundary, constant temperature Ta is fixed as corporal temperature, while adiabatic Neumann condition is applied in right boundary ($x=L$).

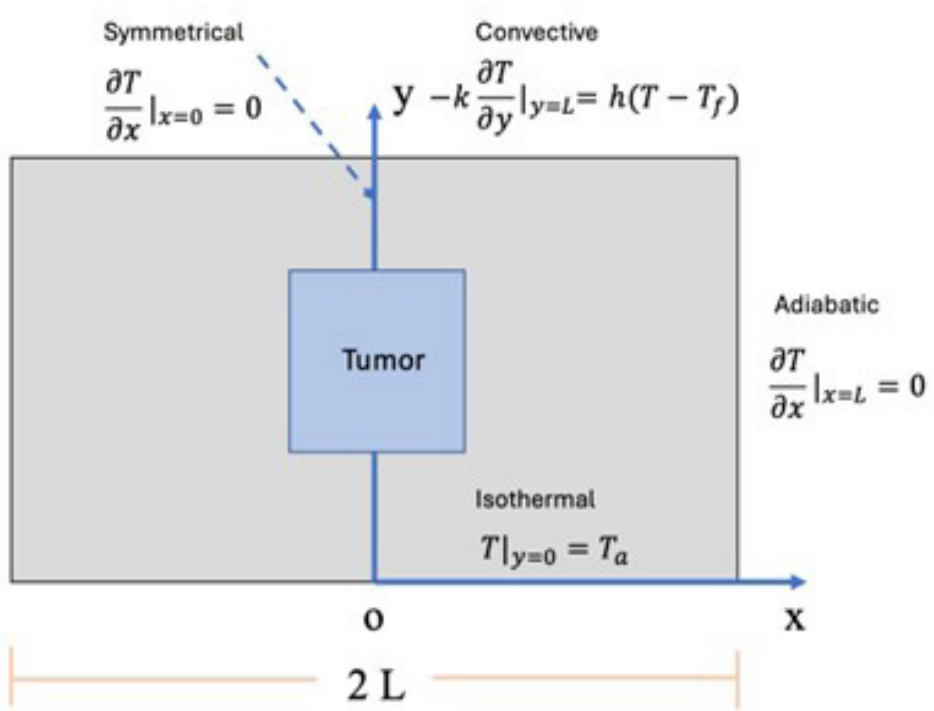

Fig 5. Domain and boundary conditions for 2D problem of heat transfer in tissue with tumor.

No irradiation heat is considered, i.e. $Qs = 0\ W/m^3$ is set in governing equation (1). Other parameters regarding heat transfer and tissue properties are presented in Table 2. With the aim of validating the LMAPS scheme for solving 2D bioheat equation, three cases are considered: tissue without tumor, with a mild tumor (Tumor 1) and with a stronger tumor (Tumor 2). Other properties are equivalent to those in the previous section. As can be seen in Table 2, the differences between healthy tissue and tumors are given by perfusion parameter ηb and metabolic heat Q_m.

TABLE 2. PARAMETERS FOR 2D PROBLEM OF TISSUE WITH TUMOR.

Parameter	Value	Unit
hconv	20	W m-2 K-1
Tf	20	°C
ηb (no tumor)	1x10-4	s-1
Qm (no tumor)	400	W m-3
ηb (Tumor 1)	1x10-3	s-1
Qm (Tumor 1)	4000	W m-3
ηb (Tumor 2)	1x10-2	s-1
Qm (Tumor 2)	40000	W m-3

Steady temperature profiles obtained with OpenFOAM and LMAPS along lines $y=L$ and $x=0$ are presented in Figure 6. Temperature increase reveals the presence of the tumor if they are compared to the case without tumor, regarding the fact that the metabolic heat and perfusion are between 10 and 100 times higher than in healthy tissue. Both numerical results have similar trends, but OpenFoam profiles show a discontinuity towards Neumann boundaries. This behavior might be attributed to the numerical implementation of the

zero-gradient condition in the cell-centered FVM with low approximation order spatial discretization schemes, which can introduce local errors at the boundary in coarse meshes. Also, x-profiles for cases without tumor and with tumor 1, present magnitude differences produced by Neumann boundary condition errors. In order to check LMAPS accuracy, a comparison with other numerical solutions is performed and shown in Figure 7 for tumor 2 case.

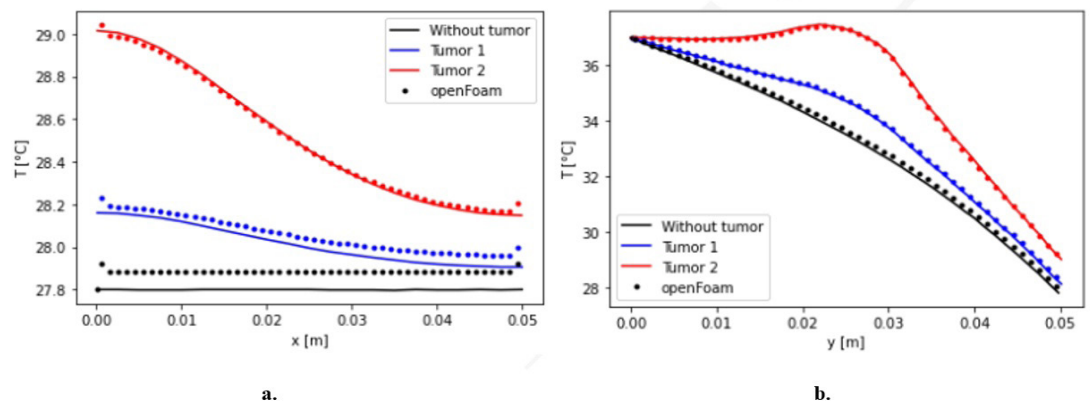

Fig 6. Numerical temperature profiles for heat transfer in two-dimensional tissue with and without tumor on a. y=L, b. x=0.

Among numerical strategies used to solve the problem with an equivalent spatial discretization, LMAPS show superior accuracy with respect to reference solution obtained by Lattice-Boltzman methods and reported in [31]. Finite element-based tools like FreeFem and Comsol, exhibit high errors in the upper boundary (Figure 7b.) where Robin boundary condition is applied. These numerical results confirm that LMAPS is a suitable method to solve bioheat equations with convective boundary conditions and multi-region domain with moderate thermophysical property differences.

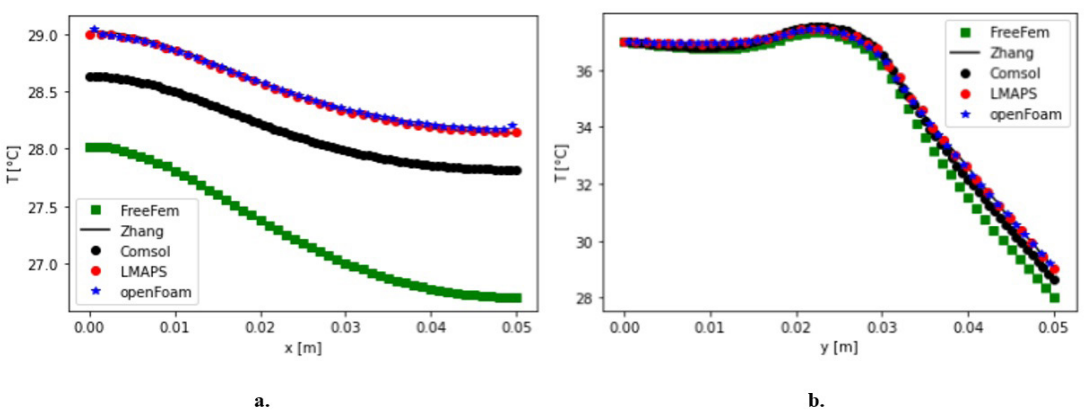

Fig 7. Numerical temperature profiles for heat transfer in two-dimensional tissue for tumor 2 case on a. y=L, b. x=0.

Temperature distribution and cell damage in a hypothetical case with a tumor

A theoretical case of PPTT application proposed by Soni et al. [32], is solved by LMAPS and OpenFOAM in order to find temperature distributions and the associated cell damage quantification. Tissue in cylindrical geometry with an embedded tumor zone as shown in Figure 8a is considered a simplified case for superficial PPTT application. Figure 8b shows a 2D domain corresponding to an axisymmetric portion of the 3D original domain where x-coordinate and z-coordinate represent, respectively, radial and axial directions. In a similar way to the previous problems, a convective heat condition is fixed in the upper boundary with h=5 W/m²/K, the body temperature is given in the right and lower border and a symmetry condition is applied in the left boundary which correspond to cylinder axis.

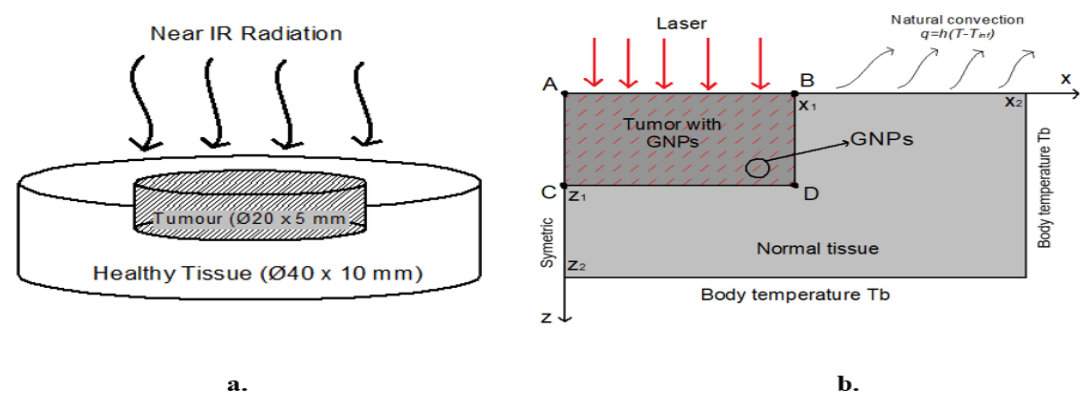

Fig 8. Theoretical tissue subjected to PPTT, a) geometric configuration, b) computational domain and boundary conditions.

In this case, equation (1) is solved with Qs given by the Beer-Lambert law, expressed by (4) whereby radial distribution of the laser is not considered according to [26]. The absorption and dispersion coefficients are equivalent to the values for healthy tissue and tumor with NPs given by the referenced authors. OpenFOAM multi-region conjugate heat transfer solver is employed to obtain the transient temperature behavior. As shown in Figure 9, the results are in good agreement with LMAPS and reference solutions. Transient behavior is depicted by Figure 9a., where temperatures at the upper-left corner (highest value) and at the lower-right corner of tumor are shown as a function of time. Also, steady temperatures values are presented on bottom, middle and upper part of tumor in Figure 9b. As it can be seen, numerical results are close to reference solution being LMAPS spatial trends more approximated than OpenFOAM ones. Although no interphase condition is imposed in LMAPS solution between healthy and tumoral tissue, a continuous solution is obtained given the higher order spatial discretization offered by the scheme. Hence, LMAPS can be used for multizone problems when there is not notorious change in thermophysical properties.

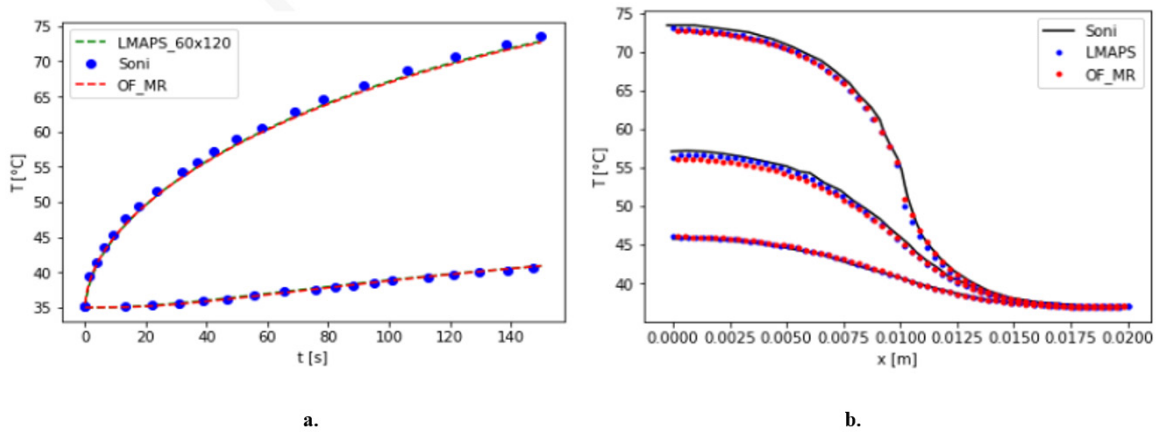

Fig 9. Temperature in tissue subjected to PPTT obtained by OpenFOAM and LMAPS: a) Transient behavior. b) Spatial profiles.

Finally, damage factor (a), computed by Arrhenius model given by equation (7) is presented in Figure 10a. Also, relative population of alive (Figure 10b) and dead cells (Figure 10c.) are estimated by expressions (8) and (9), as the three-state model used here as an alternative approach with the parameters reported by [29]. Coinciding with the results reported by the authors, the two models show a zone of damage similar in extent and corresponding to the zone of high temperature as expected. Models cannot be compared quantitively since the obtained transient behavior and the output scales are different for each of the models and, to the best of the authors' knowledge, parameter equivalence between models has not been reported. However, cell damage results show feasible application of LMAPS temperature results to PPTT simulation.

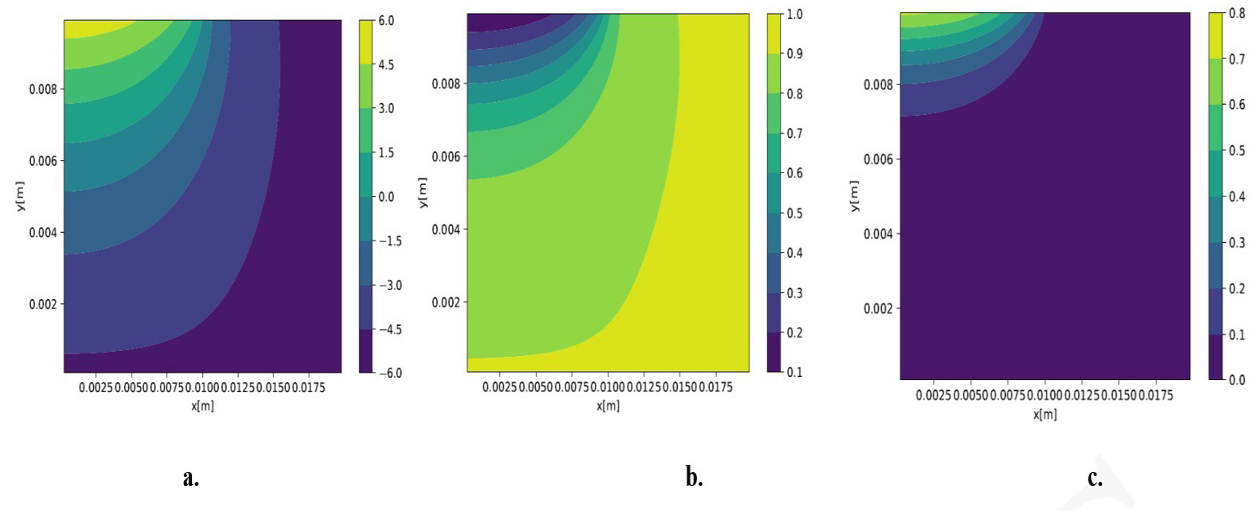

Fig 10. Cell damage results in tissue subjected to PPTT: (a) the damage factor computed with the Arrhenius model and the relative population of (b) living and (c) dead cells estimated by three-state model.

CONCLUSIONES

A numerical framework based on the meshless LMAPS has been formulated, implemented and validated with the aim of estimating cell damage caused by PPTT in 2D domains by solving bioheat equations including radiation term. The LMAPS method is validated by

comparison to computational tool OpenFOAM and reported results for benchmark problems, including analytical and numerical solutions. Regarding cell death models, results obtained with Arrhenius and Three-state methods are equivalent, however the latter can give more detail since it can compute population of vulnerable cells. The developed numerical strategy can be used to evaluate efficiency and to find suitable operational conditions for PPTT as long as tissue, tumor and nanoparticle thermophysical and optical properties, laser energy distribution and nanoparticle concentration in tissue are provided. Future work will be focused on applying the proposed method to complex geometries such as those found in clinical situations and to heterogeneous nanoparticle distributions associated with administration processes.

CRediT AUTHORSHIP CONTRIBUTION STATEMENT

J. Hurtado-Álvarez: Software, Validation, Research, Writing – Original draft, Visualization. C. Bustamante-Chaverra: Conceptualization, Methodology, Writing – Review and editing. R. Valencia-Cardona: Conceptualization, Writing – Review and editing, Visualization, Project management, Fundraising. W. Flórez-Escobar: Conceptualization, Writing – Review and editing, Supervision.

FUNDING

This work was carried out in the framework of the research project: “Alternative method based on plasmonic photothermal therapy for the treatment of gastric adenocarcinoma from an in vitro and in silico model” with the support of the direction of research and innovation of the Universidad Pontificia Bolivariana and the “Convocatoria Conjunta de Proyectos I+D+i en el Marco de la Agenda Regional I+D → I 2020” with the participation of the following external institutions: Universidad de Antioquia (UdeA), Escuela de Ingeniería de Antioquia (EIA), Institución Universitaria Pascual Bravo (I. U.Pascual Bravo) and RutaN-Medellín. Start year: 2020, end year: 2023.

REFERENCIAS

[1] S. Jain, D. G. Hirst, and J. M. O’Sullivan, “Gold nanoparticles as novel agents for cancer therapy,” *Br. J. Radiol.*, vol. 85, no. 1010, pp. 101–113, 2012, doi: 10.1259/bjr/59448833.

[2] L. Jauffred, A. Samadi, H. Klingberg, P. M. Bendix, and L. B. Oddershede, “Plasmonic Heating of Nanostructures,” *Chem. Rev.*, vol. 119, no. 13, pp. 8087–8130, 2019, doi: 10.1021/acs.chemrev.8b00738.

[3] C. D. Kaddi, J. H. Phan, and M. D. Wang, “Computational nanomedicine: Modeling of nanoparticle-mediated hyperthermal cancer therapy,” *Nanomedicine*, vol. 8, no. 8, pp. 1323–1333, 2013, doi: 10.2217/nnm.13.117.

[4] I. Raouf, S. Khalid, A. Khan, J. Lee, H. S. Kim, and M. H. Kim, “A review on numerical modeling for magnetic nanoparticle hyperthermia: Progress and challenges,” *J. Therm. Biol.*, vol. 91, p. 102644, 2020, doi: 10.1016/j.jtherbio.2020.102644.

[5] H. Pennes, “Analysis of tissue and arterial blood temperatures in the resting human forearm,” *J Appl Physiol*, vol. 1, pp. 93–148, 1962, doi: 10.5005/jp/books/12678_10.

[6] E. H. Wissler, “50 years of JAP: Pennes’ 1948 paper revisited,” *J Appl Physiol*, vol. 85, pp. 35–41, 1998.

[7] K. Das and S. C. Mishra, “Study of thermal behavior of a biological tissue: An equivalence of Pennes bioheat equation and Wulff continuum model,” *J. Therm. Biol.*, vol. 45, pp. 103–109, 2014, doi: 10.1016/j.jtherbio.2014.08.007.

[8] J. Ghazanfarian, R. Saghatchi, and D. V. Patil, “Implementation of Smoothed-Particle Hydrodynamics for non-linear Pennes’ bioheat transfer equation,” *Appl. Math. Comput.*, vol. 259, pp. 21–31, 2015, doi: 10.1016/j.amc.2015.02.036.

[9] B. Mochnacki and E. Majchrzak, "Numerical model of thermal interactions between cylindrical cryoprobe and biological tissue using the dual-phase lag equation," *Int. J. Heat Mass Transf.*, vol. 108, pp. 1–10, 2017, doi: 10.1016/j.ijheatmasstransfer.2016.11.103.

[10] I. K. Tjahjono and Y. Bayazitoglu, "Near-infrared light heating of a slab by embedded nanoparticles," *Int. J. Heat Mass Transf.*, vol. 51, no. 7–8, pp. 1505–1515, 2008, doi: 10.1016/j.ijheatmasstransfer.2007.07.047.

[11] J. Vera and Y. Bayazitoglu, "Gold nanoshell density variation with laser power for induced hyperthermia," *Int. J. Heat Mass Transf.*, vol. 52, no. 3–4, pp. 564–573, 2009, doi: 10.1016/j.ijheatmasstransfer.2008.06.036.

[12] Y. Feng et al., "Nanoshell-mediated laser surgery simulation for prostate cancer treatment," *Eng. Comput.*, vol. 25, no. 1, pp. 3–13, 2009, doi: 10.1007/s00366-008-0109-y.

[13] S. Motaei, M. Ghazavi, and G. Rezazadeh, "Incorporating temperature-dependent properties into the modeling of photo-thermo-mechanical interactions in cancer tissues", *Thermal Science and Engineering Progress*, vol. 47, pp. 102351, 2024, doi: 10.1016/j.tsep.2023.102351.

[14] X. Xu, A. Meade, and Y. Bayazitoglu, "Feasibility of selective nanoparticle-assisted photothermal treatment for an embedded liver tumor," *Lasers Med. Sci.*, vol. 28, no. 4, pp. 1159–1168, 2013, doi: 10.1007/s10103-012-1195-z.

[15] H. C. Huang, K. Rege, and J. J. Heys, "Spatiotemporal temperature distribution and cancer cell death in response to extracellular hyperthermia induced by gold nanorods," *ACS Nano*, vol. 4, no. 5, pp. 2892–2900, 2010, doi: 10.1021/nn901884d.

[16] S. Soni and R. K. Sinha, "Controlling parameters for plasmonic photothermal ablation of a tumor," *IEEE J. Sel. Top. Quantum Electron.*, vol. 22, no. 4, pp. 21–28, 2016, doi: 10.1109/JSTQE.2016.2514359.

[17] A. K. Shaw, D. Khurana, and S. Soni, "Thermal damage analysis of sub-surface soft tissue sarcoma for indocyanine green mediated photothermal cancer therapy", *Thermal Science and Engineering Progress*, vol. 46, pp. 102168, 2023, doi: 10.1016/j.tsep.2023.102168.

[18] E. J. Kansa, "Multiquadrics-A scattered data approximation scheme with applications to computational fluid-dynamics-II solutions to parabolic, hyperbolic and elliptic partial differential equations," *Comput. Math. with Appl.*, vol. 19, no. 8–9, pp. 147–161, 1990, doi: 10.1016/0898-1221(90)90271-K.

[19] R. Schaback, "Basis Function Interpolation," vol. 3, pp. 251–263, 1995.

[20] C. K. Lee, X. Liu, and S. C. Fan, "Local multiquadric approximation for solving boundary value problems," *Comput. Mech.*, vol. 30, no. 5–6, pp. 396–409, 2003, doi: 10.1007/s00466-003-0416-5.

[21] B. Šarler and R. Vertnik, "Meshfree explicit local radial basis function collocation method for diffusion problems," *Comput. Math. with Appl.*, vol. 51, no. 8 SPEC. ISS., pp. 1269–1282, 2006, doi: 10.1016/j.camwa.2006.04.013.

[22] T. J. Moroney and I. W. Turner, "A finite volume method based on radial basis functions for two-dimensional nonlinear diffusion equations," *Appl. Math. Model.*, vol. 30, no. 10, pp. 1118–1133, 2006, doi: 10.1016/j.apm.2005.07.007.

[23] P. H. Chen, C. S., Fan, C. M., & Wen, "The method of approximate particular solutions for solving certain partial differential equations," *Numer. Methods Partial Differ. Equ.*, vol. 28, no. 2, pp. 506–522, 2012, doi: 10.1002/num.20631.

[24] C. S. Chen, C. M. Fan, and P. H. Wen, "The method of approximate particular solutions for solving elliptic problems with variable coefficients," *Int. J. Comput. Methods*, vol. 8, no. 3, pp. 545–559, 2011, doi: 10.1142/S0219876211002484.

[25] K. E. Atkinson, "The numerical evaluation of particular solutions for poisson's equation," *IMA J. Numer. Anal.*, vol. 5, no. 3, pp. 319–338, 1985, doi: 10.1093/imanum/5.3.319.

[26] S. Chantasiriwan, "Cartesian grid methods using radial basis functions for solving Poisson, Helmholtz, and diffusion-convection equations," *Eng. Anal. Bound. Elem.*, vol. 28, no. 12, pp. 1417–1425, 2004, doi: 10.1016/j.enganabound.2004.08.004.

[27] C. A. Bustamante, H. Power, and W. F. Florez, "A global meshless collocation particular solution method for solving the two-dimensional Navier-Stokes system of equations," *Comput. Math. with Appl.*, vol. 65, no. 12, pp. 1939–1955, 2013, doi: 10.1016/j.camwa.2013.04.014.

[28] G. Yao, J. Kolibal, and C. S. Chen, "A localized approach for the method of approximate particular solutions," *Comput. Math. with Appl.*, vol. 61, no. 9, pp. 2376–2387, 2011, doi: 10.1016/j.camwa.2011.02.007.

[29] C. A. Bustamante, H. Power, and W. F. Florez, "An efficient accurate Local Method of Approximate Particular Solutions for solving convection-diffusion problems," *Eng. Anal. Bound. Elem.*, vol. 47, no. 1, pp. 32–37, 2014, doi: 10.1016/j.enganabound.2014.06.004.

[30] X. Zhang, and Yangjiong Wu, "High-resolution strategy for localized method of approximate particular solutions to solve unsteady Navier–Stokes problems," *Eng. Anal. Bound. Elem.*, vol. 159, no. 1, pp. 11–16, 2024, doi: 10.1016/j.enganabound.2023.11.018.

[31] H. Zhang, "Lattice Boltzmann method for solving the bioheat equation," *Phys. Med. Biol.*, vol. 53, no. 3, 2008, doi: 10.1088/0031-9155/53/3/N01.

[32] S. Soni, H. Tyagi, R. A. Taylor, and A. Kumar, "Investigation on nanoparticle distribution for thermal ablation of a tumour subjected to nanoparticle assisted thermal therapy," *J. Therm. Biol.*, vol. 43, no. 1, pp. 70–80, 2014, doi: 10.1016/j.jtherbio.2014.05.003.

[33] M. J. C. van Gemert and A. J. Welch, "Time constants in thermal laser medicine," *Lasers Surg. Med.*, vol. 9, no. 4, pp. 405–421, 1989, doi: 10.1002/lsm.1900090414.

[34] N. Sahoo, S. Ghosh, A. Narasimhan, and S. K. Das, "Investigation of non-Fourier effects in bio-tissues during laser assisted photothermal therapy," *Int. J. Therm. Sci.*, vol. 76, pp. 208–220, 2014, doi: 10.1016/j.ijthermalsci.2013.08.014.

[35] N. M. Dimitriou, A. Pavlopoulou, I. Tremi, V. Kouloulias, G. Tsigaridas, and A. G. Georgakilas, "Prediction of gold nanoparticle and microwave-induced hyperthermia effects on tumor control via a simulation approach," *Nanomaterials*, vol. 9, no. 2, 2019, doi: 10.3390/nano9020167.

[36] C. J. Greenshields, "The Open Source CFD Toolbox - Programmer's Guide," no. December. OpenCFD Ltd., United Kingdom, 2015.

[37] U. K. OpenCFD Ltd., "The Open Source CFD Toolbox - User's Guide," no. May. OpenFOAM Foundation, 2012

Juan Felipe Hurtado-Álvarez received his degree in mechanical engineering from Universidad Pontificia Bolivariana in 2022, during which he actively participated in projects and research groups working on subjects related to thermofluids and energy transition.

Carlos Andrés. Bustamante-Chaverra received the M.Sc. degree in Energy Systems and the Ph.D. degree in Engineering in the Universidad Pontificia Bolivariana (UPB), Medellín, Colombia, in 2009 and 2013, respectively. Since then, he has been working in the computational mechanics research area with the Energy and Thermodynamic group at the UPB in the Mechanical Engineering Faculty. https://orcid.org/0000-0001-6625-1804

Raúl Adolfo Valencia-Cardona. Textile Engineer, Specialization in Mechanical Design, Master in Engineering, PhD degree in Engineering. Research professor of the Faculty of Nanotechnology Engineering of the Universidad Pontificia Bolivariana, Director of the Research Group of Automatics and Design A+D. Knowledge in mathematical modeling and Computational Mechanics. https://orcid.org/0000-0002-3763-3034

Whady Felipe Flórez-Escobar is a research professor of the Faculty of Mechanical Engineering. PhD from Wessex Institute of Technology University of Wales. Leader of the Mathematical Optimization Research Group (OPTIMO). Areas of work: Mathematical Modeling and Simulation, Computational Fluid Mechanics, Applied Mathematics. https://orcid.org/0000-0003-3977-0371